

On long-term boundedness of Galerkin models

Michael Schlegel^{1,2†} and Bernd R. Noack¹

¹ Institute PPRIME, CNRS – Université de Poitiers – ENSMA, UPR 3346, Département Fluides, Thermique, Combustion, CEAT, 43, rue de l'Aérodrome, F-86036 Poitiers cedex, France

² Institut für Strömungsmechanik und Technische Akustik, Technische Universität Berlin MB1, Straße des 17. Juni 135, D-10623 Berlin, Germany

(Received 1 November 2018)

We investigate linear-quadratic dynamical systems with energy preserving quadratic terms. These systems arise for instance as Galerkin systems of incompressible flows. A criterion is presented to ensure long-term boundedness of the system dynamics. If the criterion is violated, a globally stable attractor cannot exist for an effective nonlinearity. Thus, the criterion represents a minimum requirement for a physically justified Galerkin model of viscous fluid flows. The criterion is exemplified e.g. for Galerkin systems of two-dimensional cylinder wake flow models in the transient and the post-transient regime, the Lorenz system, and for physical design of a Trefethen-Reddy Galerkin system. There are numerous potential applications of the criterion, for instance system reduction and control of strongly nonlinear dynamical systems.

1. Introduction

Focus of this paper is the a priori characterisation of the long-term behaviour of a linear-quadratic differential equation system with energy preserving quadratic term. Such a dynamical system can be obtained by the spectral discretisation of the Navier-Stokes equation. More generally, many traditional Galerkin models with orthonormal basis functions fall in this category (Fletcher 1984). Of particular interest is the long-term behaviour and attractor properties which can be ideally extracted analytically from the dynamical system. For instance, a meaningful model can be requested to have globally bounded solutions. Respective analytical methods for linear-quadratic Galerkin systems are still in their infancy. For a variety of related problems, e.g., properties of fixed points, efficient tools for dynamical system analyses (see, e.g., Guckenheimer & Holmes 1986; Khalil 2002) and tensor structure analyses have been well elaborated (see, e.g., Kolda & Bader 2009).

In this study, focus will be placed on low-order Galerkin models of the coherent flow dynamics as a simple starting point. These models are of particular interest for the understanding of the nonlinear dynamics (see, e.g., Holmes *et al.* 2012) and are key enablers of closed-loop flow control applications (see, e.g., Noack *et al.* 2011). Examples of low-order models include boundary layers (Rempfer & Fasel 1994), cylinder wakes (Deane *et al.* 1991; Noack *et al.* 2003), mixing layers (Noack *et al.* 2005; Wei & Rowley 2009), lid-driven cavities (Cazemier *et al.* 1998; Balajewicz *et al.* 2013), and supersonic diffuser flows (Willcox & Megretski 2005). However, these models tend to be fragile: Small changes of system parameters may give rise to unphysical divergent solutions, at least for a subset of initial conditions. Thus, parameter identification is a delicate task

† Author to whom correspondence should be addressed: michael.schlegel@tu-berlin.de

and a priori knowledge about the long-term behaviour of Galerkin models for all initial conditions is highly desirable.

For a priori analyses of the long-term behaviour, the optimum is represented by analytical solutions. However, the general analytical solution of a class of linear-quadratic differential equation systems, including, e.g., the Lorenz system, appears to be unrealistic within the frame of the current state of the art. In contrast, the simple analytical structure of a linear-quadratic Galerkin system provides a key enabler for the application of a rich kaleidoscope of the methodologies provided by the theory of nonlinear dynamics and control theory. One example is given by the utilisation of Lyapunov’s direct method (Lyapunov 1892). In fluid mechanics this method is adopted mainly for two purposes. Firstly, it is employed for nonlinear stability analyses of fixed points and for model-based flow control design. The methodology is well-established for linear systems (see, e.g., Kim & Bewley 2007; Sipp *et al.* 2010), and generalised for nonlinear systems (see, e.g., Aamo & Krstić 2002; Khalil 2002). Applications for Lyapunov-based flow control design are demonstrated in numerical and experimental investigations (see, e.g., Gerhard *et al.* 2003; Samimy *et al.* 2007; Schlegel *et al.* 2009, 2012). A second purpose of the direct Lyapunov method is to ensure hydrodynamic stability via the sufficient condition for a monotonically decreasing fluctuation energy (see, e.g., Joseph 1976; Drazin & Reid 1981). This leads to the identification of lower bounds for the critical Reynolds number of laminar-turbulent transition and the identification of flow structures of maximal energy growth.

However, the application range of Lyapunov’s direct method is restricted by the lack of a systematic approach for the construction of appropriate Lyapunov functions. The usage of conventional Lyapunov functions like the total kinetic energy might fail the desired purpose, e.g. to show stability for interior flows: The linear stability matrix is far from being normal over a large range of Reynolds numbers. Temporal energy growth is observed which is traced back to interactions of non-orthogonal eigenvectors (Trefethen *et al.* 1993; Schmid & Henningson 2001). The application range of Lyapunov’s direct method is enhanced for some configurations (Galdi & Padula 1990; Straughan 2004). However, the identification of strict lower bounds of flow stability is often far below the critical Reynolds number.

The difficulty of finding an appropriate Lyapunov function can partially be ascribed by the design goal, e.g. by ensuring the *global* stability of fixed points in the *whole* phase space. Instead, conditions for the existence of an arbitrary globally attractive solution are considered. In this paper, we focus on the existence of trapping regions employing Lyapunov’s direct method (Swinnerton-Dyer 2000). Coarsely stated, a trapping region is a domain in state space such that each trajectory once entered the trapping region will remain inside the trapping region for all times (Meiss 2007). In case of a (globally) attracting trapping region, all trajectories outside of the trapping region converge to the trapping region. The assumption of the existence of an attracting trapping region is connected with several other properties of dynamical systems (see figure 1). In case that an attracting trapping regions exists, the system dynamics is long-term bounded because the habitat of the long-term dynamics is represented by this trapping region. An existing (globally stable) single or multiple attractor must be embedded inside of an attracting trapping region.

The existence of an attracting trapping region can be ensured via the existence of a function which is strictly of Lyapunov function type outside of a trapping region. As a well-known example, the existence of an attracting trapping region is shown for the Lorenz system (Swinnerton-Dyer 2001). We follow this hint to investigate long-term boundedness and to estimate the extent of existing attractors. In particular, we focus

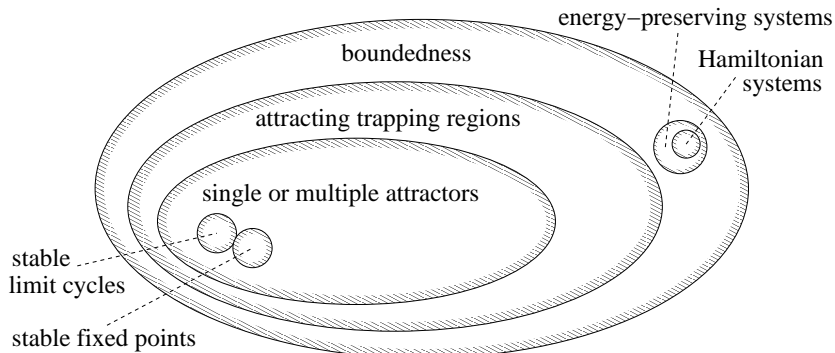


FIGURE 1. Venn diagram of dynamical systems.

on the generality for the considered class of linear-quadratic dynamical systems and the simplicity of the construction of the respective Lyapunov functions.

The content of this paper is structured as following: In section 2, the class of the considered dynamical systems is defined. In section 3, Lyapunov's direct method is generalised for the identification of trapping regions. A criterion for long-term boundedness and existence of globally stable attractors is proposed in section 4 and its range of validity is identified. Analytical and numerical application results are demonstrated for the investigation of long-term boundedness of Galerkin systems for the post-transient and transient dynamics of a two-dimensional cylinder wake flow in section 5. Moreover, a Galerkin system featuring nonlinear characteristics of the Trefethen-Reddy system is identified in section 6. The Lorenz system is investigated in section 7. In the first appendix section A, the generality of flow configurations is demonstrated, for which the Galerkin method extracts dynamical systems of the considered class. In section 8, the main findings are summarised and future directions are indicated.

2. Galerkin models of fluid flows

In this section, the considered class of dynamical systems is introduced. These systems naturally arise as Galerkin models of the incompressible Navier-Stokes equation in a steady domain Ω with stationary boundary conditions (see, e.g. Holmes *et al.* 2012). Galerkin models are typically extracted in two steps. First, a finite-dimensional Hilbert function subspace \mathcal{H} is chosen. This subspace is spanned by space dependent modes \mathbf{u}_i , $i = 1 \dots N$, which form an orthonormal basis in this Hilbert space. The flow \mathbf{u} is modelled by a Galerkin approximation with a base flow \mathbf{u}_0 and an expansion for the fluctuation $\mathbf{u}' = \mathbf{u} - \mathbf{u}_0$:

$$\mathbf{u}(\boldsymbol{\xi}, t) = \mathbf{u}_0(\boldsymbol{\xi}) + \sum_{i=1}^N x_i(t) \mathbf{u}_i(\boldsymbol{\xi}). \quad (2.1)$$

The flow state is described by the time-dependent modal amplitudes x_i . The spatial variables are denoted by $\boldsymbol{\xi}$ and the time by t . The base flow \mathbf{u}_0 might represent a steady Navier-Stokes solution or mean flow. The main purpose for the introduction of the base flow is that (2.1) satisfies the boundary conditions for arbitrary choices of modal coefficients x_i (Ladyžhenskaya 1963). The expansion modes \mathbf{u}_i , $i = 1, \dots, N$, may arise from a proper orthogonal decomposition of snapshot data or from other mathematical considerations Noack & Eckelmann (1994).

In the second step, a dynamical system is identified. At first, the Navier-Stokes equation

is projected onto the Hilbert subspace \mathcal{H} (see, e.g. Noack *et al.* 2011). As result of the modelling process, a class of dynamical systems is considered, formulated in the vector space of the state variable $\mathbf{x} = [x_1, \dots, x_N]^\top$ by

$$\frac{dx_i}{dt} = c_i + \sum_{j=1}^N l_{ij} x_j + \sum_{j,k=1}^N q_{ijk} x_j x_k \quad (2.2)$$

with the real numbers c_i, l_{ij}, q_{ijk} , for $i, j, k = 1, \dots, N$. Without loss of generality, the q_{ijk} 's are assumed to be symmetric in the last two indices, i.e.

$$q_{ijk} = q_{ikj}, \quad i, j, k = 1, \dots, N. \quad (2.3)$$

The quadratic term of (2.2) can be shown to be energy-preserving for a large class of boundary conditions (see appendix section A). This means that the sums of the quadratic coefficients over index permutations are zero

$$q_{ijk} + q_{ikj} + q_{jik} + q_{jki} + q_{kij} + q_{kji} = 2q_{ijk} + 2q_{jik} + 2q_{kij} = 0, \quad i, j, k = 1, \dots, N. \quad (2.4)$$

This property is postulated for the class of dynamical systems discussed in this paper.

The energy-preserving quadratic term has an important effect on the evolution of the fluctuation energy

$$K := \frac{1}{2} \sum_{i=1}^N x_i^2 \geq 0. \quad (2.5)$$

If \mathbf{u}_0 is the mean flow, then K denotes the standard turbulent kinetic energy (TKE) of statistical fluid mechanics. The time derivative of K reads

$$\frac{dK}{dt} = [\nabla_{\mathbf{x}} K]^\top \frac{d\mathbf{x}}{dt} = \sum_{i=1}^N x_i f_i(\mathbf{x}) = \sum_{i=1}^N c_i x_i + \sum_{i,j=1}^N l_{ij} x_i x_j, \quad (2.6)$$

i.e. the quadratic terms cancel each other out by (2.4).

Defining the vector $\mathbf{c} := [c_1, \dots, c_N]^\top$ and matrix $L := [l_{ij}]_{i,j=1}^N$, the evolution of K is given in a simple vector-matrix notation via

$$\frac{dK}{dt} = \mathbf{c}^\top \mathbf{x} + \mathbf{x}^\top L_S \mathbf{x}, \quad (2.7)$$

where the symmetric part $L_S := (L + L^\top)/2$ of L is introduced.

3. A generalisation of Lyapunov's direct method

The purpose of this section is twofold. First, a generalised Lyapunov's direct method is used to guarantee long-term boundedness of a example dynamical system without the existence of a globally stable fixed point. Second, an amplitude limiting mechanism of nonlinear dynamical systems is elaborated qualitatively and quantitatively, requiring the introduction of 'monotonically attracting trapping regions'. The long-term behaviour is characterised by the evolution of the energy of the system state with respect to the origin. For mathematical convenience and physical intuition, the energy K defined in (2.5) is chosen. This is modulo factor 1/2 the square of the Euclidean distance to the origin given by the Euclidean norm $\|\cdot\| = \sqrt{2K(\cdot)}$.

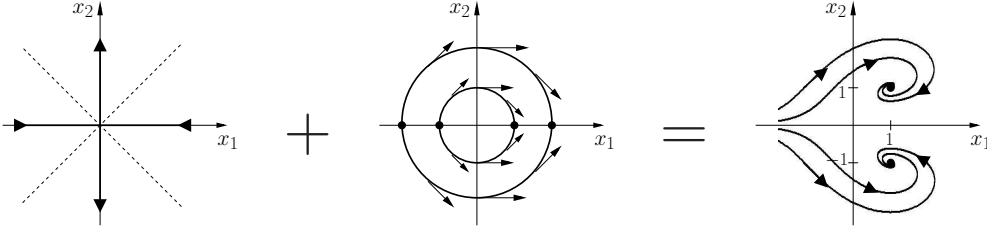


FIGURE 2. Fields of the linear term (left), the quadratic term (middle), and stable fixed point behaviour (right) of system (3.1).

3.1. Long-term boundedness of an example system

As a first example of an energy limiting mechanism, the two-dimensional system

$$\frac{dx_1}{dt} = -x_1 + x_2^2, \quad (3.1a)$$

$$\frac{dx_2}{dt} = x_2 - x_1 x_2, \quad (3.1b)$$

is considered. By the linear, symmetric part $L_S = L = \begin{bmatrix} -1 & 0 \\ 0 & 1 \end{bmatrix}$ of the two-dimensional system, the direction $[0, 1]^\top$ with positive energy growth and the direction $[1, 0]^\top$ with negative energy growth are obtained (see figure 2). The field of the quadratic term deflects the trajectories from directions of growing energy into the directions of shrinking energy. In result of the interaction of the linear and the quadratic term, all trajectories are attracted by one of the stable fixed points $[1, 1]^\top$, $[1, -1]^\top$, or along the abscissa to the origin which represents an unstable fixed point. There is no quadratic Lyapunov function by which the convergence to one of the stable fixed points can be proven a priori. The Lyapunov function does not even exist in the corresponding open half-planes of attraction. The energy is increasing or decreasing in dependence of the location of the state. There are phase-space areas of positive or negative energy growth. If the dynamics along the trajectory is dominated by negative energy growth, the system state is attracted e.g. to fixed points like in system (3.1). If the dynamics is dominated by positive energy growth, the trajectories may diverge to infinity.

By the transformation

$$\mathbf{y} = \mathbf{x} - \mathbf{m} \quad (3.2)$$

an arbitrary state $\mathbf{m} = [m_1, \dots, m_N]^\top$ can be shifted into the origin of \mathbf{y} . The fluctuation energy with respect to \mathbf{m} is defined by

$$K_{\mathbf{m}} := \sum_{i=1}^N y_i^2 = \sum_{i=1}^N (x_i - m_i)^2. \quad (3.3)$$

Its evolution is given by

$$\frac{d}{dt} K_{\mathbf{m}} = \mathbf{y}^\top A_S \mathbf{y} + \mathbf{d}^\top \mathbf{y} = (\mathbf{x} - \mathbf{m})^\top A_S (\mathbf{x} - \mathbf{m}) + \mathbf{d}^\top (\mathbf{x} - \mathbf{m}), \quad (3.4)$$

where \mathbf{d} and A_S denote the constant and linear symmetric part of the transformed Galerkin system.

Employing $\mathbf{m} = [2, 0]^\top$, the example system (3.1) is given for the shifted coordinates

by

$$\frac{dy_1}{dt} = -2 - y_1 + y_2^2, \quad (3.5a)$$

$$\frac{dy_2}{dt} = -y_2 - y_1 y_2, \quad (3.5b)$$

leading to the power balance with respect to the new origin,

$$\frac{d}{dt}K_{\mathbf{m}} = -2y_1 - y_1^2 - y_2^2. \quad (3.6)$$

Hence, the energy is growing only in a bounded domain defined by the interior of the circle given by $(y_1 + 1)^2 + y_2^2 < 1$. If $K_{\mathbf{m}}$ is large, it will decrease and the trajectories cannot escape each circle B with the origin at the centre in which the bounded domain of energy growth is contained. In conclusion, the long-term dynamics of the shifted system and consequently of the system (3.1) are bounded! Outside of each B , the energy $K_{\mathbf{m}}$ represents a strict Lyapunov function and thus Lyapunov's direct method is effective. Inside of B , the energy $K_{\mathbf{m}}$ can grow and thus Lyapunov's direct method cannot be applied.

3.2. Monotonically attracting trapping regions

For a generalisation of this approach, we introduce monotonically attracting trapping regions. A *trapping region* $D \subseteq \mathbb{R}^N$ is a compact set, in which each trajectory remains once it has entered, i.e. from $\mathbf{x}(s) \in D$ it follows that $\mathbf{x}(t) \in D$ for all $t > s$. A trapping region is termed (*globally*) *monotonically attracting*, if an energy is strictly monotonically decreasing along all trajectories starting from an arbitrary state outside of D . This implies that outside of the trapping region the energy possesses the mathematical properties of a strict Lyapunov function. For our choice of energy $K_{\mathbf{m}} = \|\mathbf{x} - \mathbf{m}\|^2/2$, it is sufficient to consider closed balls

$$B(\mathbf{m}, R) := \{\mathbf{x} \in \mathbb{R}^N : \|\mathbf{x} - \mathbf{m}\|^2 \leq R^2\} \quad (3.7)$$

with the centre \mathbf{m} and radius $0 < R < \infty$. For later reference, these closed balls are also expressed in terms of translated coordinates $\mathbf{y} = \mathbf{x} - \mathbf{m}$:

$$B_{\mathbf{y}}(R) := \{\mathbf{y} \in \mathbb{R}^N : \|\mathbf{y}\| \leq R\}. \quad (3.8)$$

Here, each closed ball containing D as a subset is a monotonically attracting trapping region as well.

If all eigenvalues of A_S are negative, i.e. $0 > \lambda_1 \geq \dots \geq \lambda_N$, then Lyapunov's direct method is effective for large deviations. This is immediately shown by the energy evolution equation (3.4). In the following, the energy evolution equation is analysed to obtain monotonically attracting trapping regions.

For that, a negative definite linear symmetric part A_S is postulated in the following. Invoking the diagonalisation

$$A_S = T^\top \Lambda T \quad (3.9)$$

of the symmetric matrix A_S with the diagonal eigenvalue matrix Λ and the orthogonal matrix T comprising the eigenvectors, a transformation

$$\mathbf{z} = T \mathbf{y} \quad (3.10)$$

is defined, preserving the energy $K_{\mathbf{m}}$. Employing this coordinate transformation (rotation

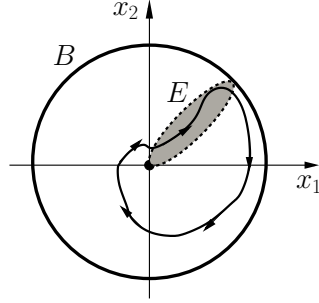


FIGURE 3. Principal sketch of boundedness of a solution of a Galerkin system (2.2) in a closed ball B . For simplicity, the origin is not shifted, i.e. $\mathbf{m} = \mathbf{0}$. The growth of energy to the origin is positive only inside of an ellipsoid E .

+ reflections), the energy growth is given by

$$\frac{d}{dt}K_{\mathbf{m}} = \sum_{i=1}^N h_i z_i + \lambda_i z_i^2 = \sum_{i=1}^N \lambda_i \left(z_i + \frac{h_i}{2} \right)^2 - \sum_{i=1}^N \lambda_i \frac{h_i^2}{4}. \quad (3.11)$$

with the components h_i of $\mathbf{h} := \mathbf{d} \mathbf{T}^\top$.

For $\mathbf{d} = \mathbf{0}$ and hence $\mathbf{h} = \mathbf{0}$, the energy is a strict Lyapunov function since $\lambda_i < 0$, $i = 1, \dots, N$, has been assumed. In addition, a globally stable fixed point is situated at the origin. For $\mathbf{d} \neq \mathbf{0}$ and hence $\mathbf{h} \neq \mathbf{0}$, the energy growth can be positive close to the origin. In more detail, the sign of the energy growth is changing at the boundary of an ellipsoid E which is defined via

$$\sum_{i=1}^N \frac{1}{\alpha_i^2} \left(z_i + \frac{h_i}{2} \right)^2 = 1 \quad \text{with} \quad \alpha_i := \sqrt{\frac{\sum_{j=1}^N \lambda_j h_j^2}{4 \lambda_i}}. \quad (3.12)$$

In the interior of the ellipsoid E , the energy growth is positive with a maximum growth at the centre $-\mathbf{h}/2$. Outside of the ellipsoid the energy is decreasing. At the boundary, the energy stays constant. Note, that the origin is situated at the boundary of the ellipsoid because it is trivially solving equation (3.12). The half-axes α_i are directly proportional to the Euclidean norm of \mathbf{h} and hence of \mathbf{d} .

After a finite time, the system state is trapped in the smallest closed ball B with centre at the origin of the \mathbf{y} -coordinates such that the ellipsoid E is contained[†]. Hence, the smallest monotonically attracting trapping ball is given by B !

The long-term behaviour of the system, represented e.g. by an globally stable attractor, is either part of the boundary without growth of $K_{\mathbf{m}}$, or is alternating between positive energy growth inside of E and negative energy growth in $B \setminus E$ (see figure 3). The case $\mathbf{d} = \mathbf{0}$ can be seen as a degeneration of E and B to the fixed point at the origin.

4. A sufficient criterion for long-term boundedness

In this section, a sufficient criterion for long-term boundedness of Galerkin systems is derived to exclude infinite blow ups of the system state $\mathbf{x}(t)$ in finite or infinite periods of time. Via the criterion of theorem 1 below, the existence of monotonically attracting trapping regions is considered. For the generic class of Galerkin systems (2.2) with effective nonlinearity, it is shown that a globally stable attractor can only exist if there is

[†] Only in the non-generic case, that there is a stable fixed point at the intersection of the boundaries of B and E , it might take infinite time to enter B .

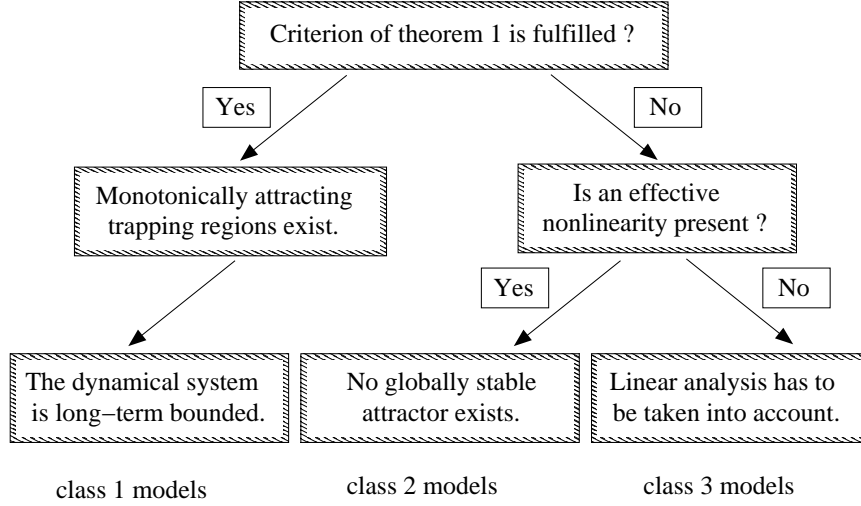


FIGURE 4. Decision tree diagram for long-term boundedness of linear-quadratic systems.

a monotonically attracting trapping region. The results of this section will culminate in the procedure sketched in figure 4, guiding the determination of the long-term behaviour of the Galerkin systems (2.2).

To keep the notation simple, the following vector-matrix representation of (2.2) is employed using the symmetric matrices $Q^{(\alpha)} := [q_{\alpha ij}]_{i,j=1}^N$, $\alpha = 1, \dots, N$,

$$\frac{d\mathbf{x}}{dt} = \mathbf{c} + L\mathbf{x} + \left[\mathbf{x}^\top Q^{(1)} \mathbf{x}, \dots, \mathbf{x}^\top Q^{(N)} \mathbf{x} \right]^\top. \quad (4.1)$$

Using this nomenclature, the condition (2.4) can be rewritten as

$$q_{jk}^{(i)} + q_{ik}^{(j)} + q_{ij}^{(k)} = 0, \quad i, j, k = 1, \dots, N \quad (4.2)$$

employing the elements $q_{jk}^{(i)}$, $j, k = 1, \dots, N$ of the symmetric matrices $Q^{(i)}$.

For the translated variable $\mathbf{y} = \mathbf{x} - \mathbf{m}$, the dynamical system

$$\frac{d\mathbf{y}}{dt} = \mathbf{d} + A\mathbf{y} + \left[\mathbf{y}^\top Q^{(1)} \mathbf{y}, \dots, \mathbf{y}^\top Q^{(N)} \mathbf{y} \right]^\top \quad (4.3)$$

with

$$\mathbf{d} := \left(c_i + \sum_{j=1}^N l_{ij} m_j + \sum_{j,k=1}^N q_{ijk} m_j m_k \right)_{i=1}^N \quad (4.4)$$

and

$$A := \left(l_{ij} + \sum_{k=1}^N (q_{ijk} + q_{ikj}) m_k \right) \quad (4.5)$$

is obtained. Note that the symmetric part A_S of A can be represented as a linear combination of the symmetric part L_S of L and of the $Q^{(i)}$'s

$$A_S := \frac{1}{2} (A + A^\top) = L_S + \sum_{i=1}^N m_i Q^{(i)}, \quad (4.6)$$

exploiting the symmetry properties (2.4) and (2.3).

Employing the translation, a simple condition for the existence of a monotonically attracting trapping region can be found. If all eigenvalues of A_S are negative, i.e. $0 > \lambda_1 \geq \dots \geq \lambda_N$, then the energy evolution equation is transformed to equation (3.11) employing the rotation of the coordinate system to the principal axes. Hence, the domain of energy growth is identified to be inside of the ellipsoid given by (3.12). Every ball with the origin $\mathbf{y} = \mathbf{0}$ at the centre, which contains the ellipsoid, is a monotonically attracting trapping region. Consider the estimate

$$\alpha_i \leq \sqrt{\frac{\lambda_N}{4\lambda_1}} \|\mathbf{d}\|, \quad (4.7)$$

invoking the definition (3.12) of the half-axes α_i . Then a radius of such a ball, not necessarily the infimum amongst such radii, is given by $R_m = \sqrt{\lambda_N/\lambda_1} \|\mathbf{d}\|$.

On the other hand, given a monotonically attracting trapping region, the distance of every state \mathbf{x} outside the trapping region to a state \mathbf{m} inside of the trapping region is monotonically decreasing by definition. This is only true if the right-hand side of the power balance (3.4) is negative for an \mathbf{m} inside the trapping region and if the energy $K_{\mathbf{m}}$ is large enough. By symmetry considerations this requires that all eigenvalues of A_S are negative.

The above-mentioned results are summarised in the following theorem

THEOREM 1. MONOTONICALLY ATTRACTING TRAPPING REGIONS

Regarding the system (4.1), the following two statements are equivalent:

(a) *There is a monotonically attracting trapping region.*

(b) *There is an \mathbf{m} , such that there are only negative eigenvalues $0 > \lambda_1 \geq \dots \geq \lambda_N$ of the symmetric linear part A_S (4.6) of the shift-transformed system (4.3).*

If these conditions are true, $R_m = \sqrt{\lambda_N/\lambda_1} \|\mathbf{d}\|$ is a radius such that $B(\mathbf{m}, R_m)$ is a monotonically attracting trapping region.

In conclusion, a sufficient condition for the long-term boundedness of systems (4.1) over an infinite time horizon has been found.

As a first example of an application of the criterion, we show the existence of a monotonically attracting trapping region for the system (3.1). It can be written in the form of equation (4.1) with

$$\mathbf{c} = \begin{bmatrix} 0 \\ 0 \end{bmatrix}, L = \begin{bmatrix} -1 & 0 \\ 0 & 1 \end{bmatrix}, Q^{(1)} = \begin{bmatrix} 0 & 0 \\ 0 & 1 \end{bmatrix}, Q^{(2)} = \begin{bmatrix} 0 & -\frac{1}{2} \\ -\frac{1}{2} & 0 \end{bmatrix}. \quad (4.8)$$

Considering the translation with $\mathbf{m} = [2, 0]^\top$, and invoking (4.6), the symmetric part of the transformed system is

$$A_S = \begin{bmatrix} -1 & 0 \\ 0 & -1 \end{bmatrix}.$$

By the negative definiteness of A_S , the existence of a monotonically attracting trapping region is shown. One of these regions is given by the closed ball $B_{\mathbf{y}}(2)$ in the \mathbf{y} -coordinates (see (3.8)) and equivalently by $B(\mathbf{m}, 2)$ in the \mathbf{x} -coordinates (see (3.7)). All solutions, given by the stable and unstable fixed points are situated inside of B and at the boundary of the ellipsoid E defined by equation (3.12), along which the energy $K_{\mathbf{m}}$ is maintained.

Although boundedness of a large class of systems is ensured, there might exist long-term bounded systems even with a globally stable fixed point which do not fit the condition of theorem 1. One class is given by Hamiltonian systems in which the energy $K_{\mathbf{m}}$ is preserved. Here, $A_S = \mathbf{0}$, because the distance to an \mathbf{m} of the initial values remains constant for all times. All trajectories are embedded in invariant spaces, representing shells

of constant distance around the centre. Hence the dynamics are bounded, but globally stable trapping regions or even a globally stable attractor do not exist.

Another class is given from the linear system behaviour of (4.1) with vanishing nonlinear term $\mathbf{Q}^{(i)} = \mathbf{0}$, $i = 1, \dots, N$, $\mathbf{c} = \mathbf{0}$, and a non-normal matrix L . Here, an attracting behaviour can be accompanied with temporal energy growth as known from the theory of non-normal matrices (Trefethen & Embree 2005). Even if there is a globally stable fixed point, the convergence of the trajectories can be non-monotonous with alternating increase and decrease of the distance to the fixed point.

However in the generic case of an effective nonlinearity, each globally non-monotonically attracting set is embedded in a larger monotonically attracting trapping region. To introduce the notion of an *effective nonlinearity*, a reformulation of the transformed system (4.3) is considered. Let $r := \|\mathbf{y}\| > 0$ be the amplitude (radius) of the state and $\mathbf{w} := \mathbf{y}/r$ the ‘generalised phase’ (direction) on the unit ball $\partial B_{\mathbf{y}}(1)$. It yields

$$\frac{d\mathbf{w}}{dt} = \frac{1}{r}\mathbf{d} + A\mathbf{w} + r \left[\mathbf{w}^\top \mathbf{Q}^{(1)} \mathbf{w}, \dots, \mathbf{w}^\top \mathbf{Q}^{(N)} \mathbf{w} \right]^\top, \quad (4.9a)$$

$$\frac{dr}{dt} = \mathbf{d}^\top \mathbf{w} + r \mathbf{w}^\top A_S \mathbf{w}. \quad (4.9b)$$

The focus of interest is on large distances r from the origin \mathbf{m} . The nonlinearity is termed effective if the constant and linear term of the phase equation (4.9a) can be neglected for large r

$$\frac{d\mathbf{w}}{dt} = r \left[\mathbf{w}^\top \mathbf{Q}^{(1)} \mathbf{w}, \dots, \mathbf{w}^\top \mathbf{Q}^{(N)} \mathbf{w} \right]^\top, \quad (4.10)$$

i.e. the trajectories are driven by the dynamics of the equations (4.10) and (4.9b). Generically, the spatial asymptotical behaviour of the considered Galerkin systems (2.2) is described by these two equations. However, this is not true if there exist invariant manifolds of (4.1) with vanishing quadratic term, i.e. $\mathbf{x}^\top \mathbf{Q}^{(i)} \mathbf{x} = \mathbf{0}$ for all corresponding states. Here, linear analyses have to be applied in addition to identify the long-term behaviour conclusively. For illustration, a corresponding example is detailed in subsection B.2 of the appendix section B.

For effective nonlinearity, the dynamics of large deviations is independent from the antisymmetric part of the linear term: the dynamics of the phase \mathbf{w} is determined solely by the quadratic term, the dynamics of r solely by the symmetric part of the linear term and the constant term. The mechanisms for temporal energy growth resulting from non-orthogonal eigendirections of non-normal matrices are excluded for large r . It can be concluded for each attracting trapping region, that it is embedded in a monotonically attracting trapping region.

These results are summarised in the following theorem.

THEOREM 2. TRAPPING REGIONS

Consider a system (4.1) with effective nonlinearity, i.e. the dynamics of large deviations of the shifted system (4.3) can be described by (4.9b) and (4.10). Then each (globally) attracting trapping region is contained in a monotonically attracting trapping region. In particular, the existence of a monotonically attracting trapping region is necessary for the existence of a globally stable attractor.

In conclusion, the long-term behaviour is determined via application of the procedure illustrated in figure 4. For the criterion of theorem 1, N components of \mathbf{m} have to be found such that the N eigenvalues of A_S given by (4.6) are negative. While this can be analytically done for systems of dimension lower than or equal to four, for larger

dimensions numerical linear algebra and multidimensional optimisation like simulated annealing has to be employed.

5. Long-term boundedness of Galerkin models for cylinder wake flows

In this section, we investigate the long-term boundedness of a hierarchy of Galerkin models for periodic cylinder wakes (Noack *et al.* 2003). The considered systems include a 3-dimensional mean-field system (subsection 5.1), an 8-dimensional POD model (subsection 5.2) and a 9-dimensional generalisation of this POD model with a stabilising shift mode (subsection 5.3). The existence of a monotonically attracting trapping region is demonstrated analytically for the mean-field system which is known to have a globally stable limit cycle. The corresponding existence is also numerically shown for the 9-dimensional model which generalises the mean-field system by inclusion of the 2nd to 4th harmonics. The existence of a monotonically attracting trapping region is disproved for the 8-dimensional system which has a locally stable limit cycle but also solutions converging to infinity. Thus, the theorems of section 4 proof numerically suggested behaviour of the hierarchy of Galerkin models.

5.1. On the long-term boundedness of a mean-field system

We consider a mean-field system for a soft onset of oscillatory fluctuations (Noack *et al.* 2003) in fluid flows. The state contains 3 coordinates: x_1 and x_2 describe the amplitude of the phase of the oscillatory fluctuation and x_3 characterises the mean-field deformation. The origin $x_1 = x_2 = x_3 = 0$ corresponds to the steady solution. For simplicity, many parameters of the general mean-field model (see, e.g., Noack *et al.* 2011) are set to zero or unity, following Sec. 2.1 of Noack *et al.* (2003). Only the bifurcation parameter μ is left. The resulting mean-field system reads

$$\frac{dx_1}{dt} = \mu x_1 - x_2 - x_1 x_3, \quad (5.1a)$$

$$\frac{dx_2}{dt} = \mu x_2 + x_1 - x_2 x_3, \quad (5.1b)$$

$$\frac{dx_3}{dt} = -x_3 + x_1^2 + x_2^2. \quad (5.1c)$$

and has the form of system (2.2) with an energy-preserving quadratic term. For subcritical Reynolds numbers ($\mu < 0$), the system has a globally stable fixed point $x_1 = x_2 = x_3 = 0$. For supercritical values, ($\mu > 0$) these fixed points becomes unstable and all trajectories converge to the limit cycle

$$x_1 = \sqrt{\mu} \cos(t), \quad x_2 = \sqrt{\mu} \sin(t), \quad x_3 = \mu. \quad (5.2)$$

modulo an irrelevant phase. This limit cycle represents vortex shedding.

This differential equation system can be brought in the form (4.1) with

$$\mathbf{c} = \begin{bmatrix} 0 \\ 0 \\ 0 \end{bmatrix}, \quad L = \begin{bmatrix} \mu & -1 & 0 \\ 1 & \mu & 0 \\ 0 & 0 & -1 \end{bmatrix} \quad (5.3)$$

and

$$Q^{(1)} = \begin{bmatrix} 0 & 0 & -\frac{1}{2} \\ 0 & 0 & 0 \\ -\frac{1}{2} & 0 & 0 \end{bmatrix}, \quad Q^{(2)} = \begin{bmatrix} 0 & 0 & 0 \\ 0 & 0 & -\frac{1}{2} \\ 0 & -\frac{1}{2} & 0 \end{bmatrix}, \quad Q^{(3)} = \begin{bmatrix} 1 & 0 & 0 \\ 0 & 1 & 0 \\ 0 & 0 & 0 \end{bmatrix},$$

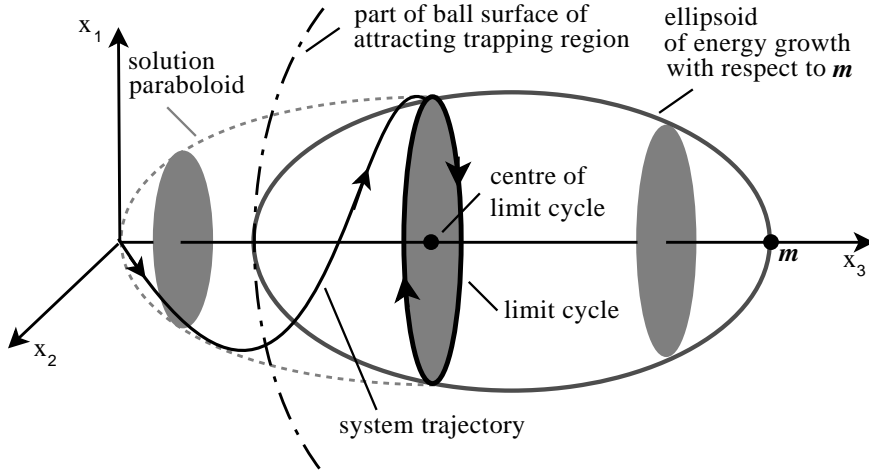


FIGURE 5. Solution behaviour of the system (5.1). The trajectories converge in spirals along the paraboloid (light grey, dashed line) toward the globally stable limit cycle (black, solid and thick line), as exemplified by one representative (black, solid, thin line). For one \mathbf{m} with a corresponding negative definite A_S the trapping region of minimal radius (indicated by black, dot-dashed line) is determined by the contained ellipsoid of positive energy growth (3.12) (dark grey, solid, thick line).

with a real parameter $\mu > 0$.

It may be interesting to note that system (3.1) originated from the mean-field model (5.1) with $\mu = 1$. The component x_1 in (3.1) corresponds to the component x_3 in (5.1), the state x_2 in (3.1) to the amplitude $\sqrt{x_1^2 + x_2^2}$ of the two first components in (5.1). Like in the example system (3.1), there are areas in which the amplitude of the oscillation in the x_1 - x_2 -plane grows while the x_3 -direction has only negative distance growth. The stabilisation of the limit cycle can be described by the Landau equation (Noack *et al.* 2003). Like for system (3.1), the boundedness of the mean-field dynamics cannot be derived from a quadratic Lyapunov function.

The criterion of theorem 1 can easily be satisfied. Consider the translation with $\mathbf{m} = [0, 0, \mu + \epsilon]^T$ for an $\epsilon > 0$. Employing moreover (4.6), the symmetric part of the transformed system is derived to be

$$A_S = \begin{bmatrix} -\epsilon & 0 & 0 \\ 0 & -\epsilon & 0 \\ 0 & 0 & -1 \end{bmatrix}.$$

The negative definiteness of A_S implies the existence of a monotonically attracting trapping region. Following theorem 1, one of these regions is given by the closed ball $B(\mathbf{m}, R_m)$, where $R_m = (\mu + \epsilon)/\sqrt{\epsilon}$. Hence, the trapping region will grow to infinity for $\epsilon \rightarrow 0$. The limit cycle is situated inside of B and at the boundary of the ellipsoid E defined by equation (3.12), along which the energy $K_{\mathbf{m}}$ is constant. This is illustrated in figure 5. We employ that \mathbf{m} lies on the x_3 -axis orthogonal to the limit cycle plane, $K_{\mathbf{m}}$ is seen to remain constant on the limit cycle. The limit cycle is contained in the intersection set of the infinite number of ellipsoids, each defined by a positive parameter $\epsilon > 0$.

5.2. On the long-term boundedness of a POD Galerkin model

In Deane *et al.* (1991) and Noack *et al.* (2003), a Galerkin model for the cylinder wake flow is proposed employing the first 8 modes from a proper orthogonal decomposi-

tion (POD). The post-transient dynamics of oscillatory laminar vortex shedding at a Reynolds number of $Re = 100$ in the wake is accurately resolved by this model.

The 8-dimensional Galerkin system is given by the differential equation

$$\frac{dx_i}{dt} = c_i + \sum_{j=1}^8 l_{ij} x_j + \sum_{j,k=1}^8 q_{ijk} x_j x_k. \quad (5.4)$$

The energy preservation property (2.4) is enforced for the quadratic term. The kinetic energy K is produced in the first mode pair (x_1, x_2) with the same positive growth rate of energy. The other six modes form pairs of the same negative energy growth rate, consuming the energy transferred by the first pair. For initial conditions close to the projection of the Navier-Stokes attractor onto the 8-dimensional subspace, the post-transient dynamics is reproduced (Noack *et al.* 2003). Starting far from the limit cycle, also solutions which converge to infinity are numerically observed.

To test the criterion of theorem 1, the largest eigenvalue of the linear symmetric part A_S is minimised over a set of shift vectors \mathbf{m} . The optimisation has been performed via a simulated annealing algorithm (see, e.g., Gershenfeld 2006) with random seeding in $\mathbf{m} \in [-100, 100]^8$. This box contains the limit cycle which is centred around the origin. The box can be considered as very large, since it is almost two orders of magnitude larger than the radius of this limit cycle. In all computations, the minimum of the largest eigenvalues is positive, which indicates that the criterion cannot be fulfilled. This result is confirmed by simulations shown in Noack *et al.* (2003) verifying a divergent behaviour of (5.4) to infinity for some initial values. Also Deane *et al.* (1991) report fragile Galerkin system behaviour for a similar POD wake model. In fact, the fragility of the POD model for vortex shedding has inspired numerous enhancements of the reduced-order modelling method, e.g. a nonlinear eddy viscosity term (Cordier *et al.* 2013), a stabilising spectral viscosity term (Sirisup & Karniadakis 2004), a stabilising linear term (Galletti *et al.* 2004), a stabilising additional shift mode (Noack *et al.* 2003), or the inclusion of Navier-Stokes constraints construction of generalised POD modes (Balajewicz *et al.* 2013).

5.3. On the long-term boundedness of a POD Galerkin model with shift mode

The 8-dimension POD model of the previous section is stabilised by including an additional shift mode \mathbf{u}_9 in the Galerkin expansion following Noack *et al.* (2003, 2005). This shift mode \mathbf{u}_9 represents the normalised difference of mean flow and stationary solution. In addition, the base flow \mathbf{u}_0 is chosen to be the unstable steady solution so that the origin is the fixed point of the Navier-Stokes dynamics. In the following, long-term boundedness of the resulting 9-mode Galerkin system is proven for all initial conditions.

The dynamical system (5.4) is generalised by additional terms on the right-hand sides

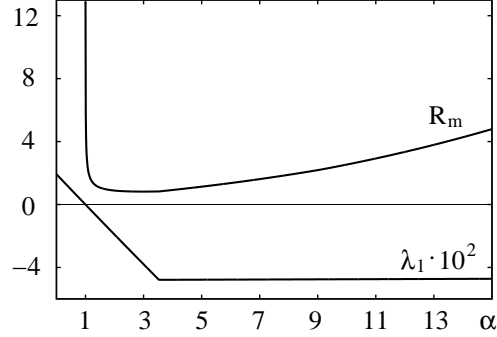


FIGURE 6. Visualisation of the criterion of theorem 1 for long-term boundedness of the 9-mode cylinder wake Galerkin system (5.5). Shown are the largest eigenvalue λ_1 of A_S of the shifted system (4.3) and the estimated radius R_m of the globally attracting trapping ball B described in this theorem, for several shift vectors $\mathbf{m} = (0, 0, 0, 0, 0, 0, 0, 0, \alpha)^\top$ with $\alpha > 0$.

and a new additional equation arising from the shift mode:

$$\frac{dx_i}{dt} = \underbrace{c_i + \sum_{j=1}^8 l_{ij} x_j + \sum_{j,k=1}^8 q_{ijk} x_j x_k}_{\text{terms from the 8-mode system (5.4)}} + \underbrace{l_{i9} x_9 + \sum_{k=1}^8 q_{i9k} x_9 x_k + \sum_{j=1}^8 q_{ij9} x_j x_9 + q_{i99} x_9^2}_{\text{additional 'shift mode' terms}}, \quad i = 1, \dots, 8, \quad (5.5a)$$

$$\frac{dx_9}{dt} = c_9 + \sum_{j=1}^9 l_{9j} x_j + \sum_{j,k=1}^9 q_{9jk} x_j x_k. \quad (5.5b)$$

For all numerically investigated initial conditions employed in Noack *et al.* (2003), the system solutions are long-term bounded and converge to a limit cycle.

In the following, we prove long-term boundedness of the 9-mode Galerkin system with the criterion of theorem 1. Learning from the mean-field model, only translations (3.2) along the mean-field axis are considered, i.e. $\mathbf{m} = (0, 0, 0, 0, 0, 0, 0, 0, \alpha)^\top$ with $\alpha > 0$. Figure 6 visualises the situation at $\alpha \approx 1$. There is a change of the sign of the largest eigenvalue of A_S from being positive to negative at $\alpha \approx 1$. By the translation, the largest eigenvalue decreases initially linearly with α . After some value of α , this largest eigenvalue remains negative and constant due other eigenvalues which are not affected by the translation. Thus, the largest eigenvalue of A_S remains constant for larger α . In conclusion, there exist translations which make A_S negative definite. Thus, the 9-mode Galerkin system is shown to be long-term bounded because a monotonically attracting trapping region must exist according to theorem 1. Furthermore, it is shown in the figure that there is a minimum of the volume of the trapping region for a certain \mathbf{m} as indicated by the curve of the estimated radius R_m of the trapping region.

6. Design of a Trefethen-Reddy Galerkin system

In this section, we consider the Trefethen-Reddy system (Trefethen *et al.* 1993) as celebrated paradigm for linear transient growth and nonlinear dynamics. This system

has a non-algebraic nonlinearity, i.e. it cannot be obtained from a Galerkin method. Here, we use the criterion of theorem 1 to design an energy-preserving quadratic term with similar nonlinear behaviour.

Trefethen *et al.* (1993) have proposed a simple dynamical system exhibiting important features of the non-normal linear term and nonlinearity:

$$\frac{d\mathbf{x}}{dt} = \begin{bmatrix} -Re^{-1} & 1 \\ 0 & -2Re^{-1} \end{bmatrix} \mathbf{x} + \|\mathbf{x}\| \begin{bmatrix} 0 & -1 \\ 1 & 0 \end{bmatrix} \mathbf{x}. \quad (6.1)$$

Here, Re mimics the effect of the Reynolds number. The linear part of this Trefethen-Reddy system is represented by a non-normal matrix such that transient growth of the energy K can be obtained in the linear regime. The transient growth levels increase with Re . At sufficiently large values, the nonlinear term becomes important and the following bootstrapping effect has been observed. Initial conditions $\mathbf{x}(0) = [0, const.]^\top$ are numerically considered. For small $\|\mathbf{x}(0)\|$, the dynamics converge to the origin with linear growth rates. For larger $\|\mathbf{x}(0)\|$, the trajectories converge to fixed points \mathbf{x}_S , $\|\mathbf{x}_S\| \approx 1$, with far larger growth rates than in the linear regime.

The Trefethen-Reddy system qualitatively displays important non-normal linear and nonlinear effects observed, for instance, in boundary layers and internal flows. However, (6.1) cannot be obtained from a Galerkin method. There exist no spatial modes $\mathbf{u}_1, \mathbf{u}_2$ such that the projection onto the incompressible Navier-Stokes equation yields a square root expression like $\|\mathbf{x}\|$.

The goal in this section is to model the bootstrapping effect by a long-term bounded Galerkin system of form (2.2), thus offering an alternative to (6.1) which is arguably more physical. Hence, a new nonlinear term needs to be identified. The requested energy preservation of the quadratic term strongly limits the number of free parameters from 10 to 2 (see also Bourgeois *et al.* 2013). The corresponding dynamical system reads

$$\frac{d\mathbf{x}}{dt} = \begin{bmatrix} -Re^{-1} & 1 \\ 0 & -2Re^{-1} \end{bmatrix} \mathbf{x} + \delta \left(\sin \theta \begin{bmatrix} x_1 & x_2 \\ -x_1^2 & \end{bmatrix} + \cos \theta \begin{bmatrix} -x_2^2 \\ x_1 & x_2 \end{bmatrix} \right) \quad (6.2)$$

for some $\delta > 0$ and $\theta \in (0, 2\pi]$. This system is of form (4.1) with

$$L_S = \begin{bmatrix} -Re^{-1} & 1/2 \\ 1/2 & -2Re^{-1} \end{bmatrix},$$

and

$$Q^{(1)} = \delta \begin{bmatrix} 0 & 2^{-1} \sin \theta \\ 2^{-1} \sin \theta & -\cos \theta \end{bmatrix}, \quad Q^{(2)} = \delta \begin{bmatrix} -\sin \theta & 2^{-1} \cos \theta \\ 2^{-1} \cos \theta & 0 \end{bmatrix}.$$

The existence of a monotonically attracting trapping region can be shown for the parameters $\theta \approx \pi/2, \pi, 3\pi/2, 2\pi$ as follows. For the translation vector

$$\mathbf{m} = \delta^{-1} [\sin \theta, \cos \theta]^\top,$$

it yields

$$A_S = \begin{bmatrix} -Re^{-1} + 2^{-1} \sin 2\theta & 0 \\ 0 & -2Re^{-1} + 2^{-1} \sin 2\theta \end{bmatrix} \approx \begin{bmatrix} -Re^{-1} & 0 \\ 0 & -2Re^{-1} \end{bmatrix}.$$

At large Reynolds number Re , the same \mathbf{m} can be employed to show the long-term boundedness for $\theta \in [\pi/2, \pi]$ and $\theta \in [3\pi/2, 2\pi]$. Via a detailed analysis of A_S for arbitrary \mathbf{m} (see the techniques applied in the appendix section B), it can be shown that the criterion of theorem 1 cannot be fulfilled for sufficient large Re and $\theta \in (0, \pi/2)$ or

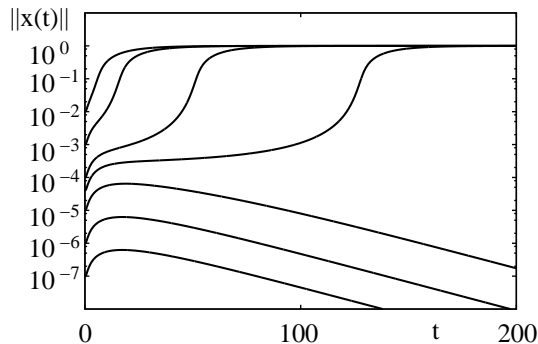


FIGURE 7. Bootstrapping effect of the modified Trefethen-Reddy system. The evolution of $\|\mathbf{x}(t)\|$ is visualised for solutions of (6.3) with initial conditions $x_1(0) = 0$, $x_2(0) = 10^{-7}, 10^{-6}, 10^{-5}, 4 \times 10^{-5}, 10^{-4}, 10^{-3}, 10^{-2}$ and for $\delta = 12.5$.

$\theta \in (\pi, 3\pi/2)$. Hence, only a $\theta \in [\pi/2, \pi]$ or $\theta \in [3\pi/2, 2\pi]$ represents a candidate to model flow attractor behaviour.

With the initial conditions of Trefethen *et al.* (1993), a similar bootstrapping effect can be observed, for instance for $\theta = 3\pi/2$ (see figure 7). For this angle, the modified Trefethen-Reddy system reads

$$\frac{dx_1}{dt} = -Re^{-1} x_1 + x_2 - \delta x_1 x_2, \quad (6.3a)$$

$$\frac{dx_2}{dt} = -2 Re^{-1} x_2 + \delta x_1^2. \quad (6.3b)$$

The location of the fixed points scale with the parameter δ . For a similar scaling like in Trefethen *et al.* (1993), $\delta = 12.5$ is chosen for the computations illustrated in figure 7.

In conclusion, the interval of system parameters for θ is reduced employing the criterion of theorem 1. The dynamical behaviour of the modified system coincides qualitatively with the original Trefethen-Reddy system: the bootstrapping effect is modelled via a dynamical system with the same linear term but an energy-preserving quadratic term. Contrary to the original model, such a system may arise from a Galerkin projection of a 2-mode expansion onto the Navier-Stokes equation.

7. Long-term boundedness of the Lorenz system

The existence of a monotonically attracting trapping region is demonstrated for Galerkin systems (2.2) with stable fixed point behaviour of the example system (3.1) and the stable periodic limit cycle dynamics of system (5.1). In this section and appendix B, more complex examples are considered. We start with the well-known Lorenz system

$$\frac{dx_1}{dt} = -\sigma x_1 + \sigma x_2, \quad (7.1a)$$

$$\frac{dx_2}{dt} = \rho x_1 - x_2 - x_1 x_3, \quad (7.1b)$$

$$\frac{dx_3}{dt} = -\beta x_3 + x_1 x_2, \quad (7.1c)$$

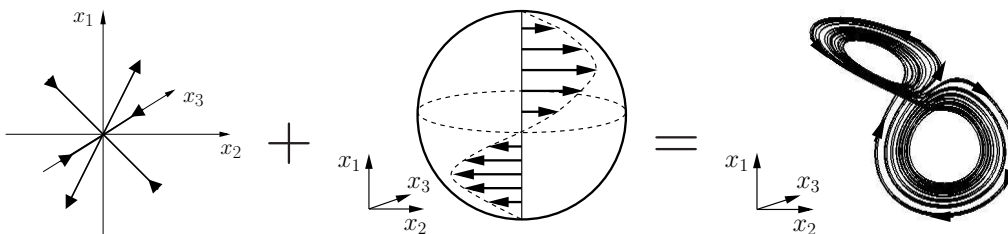


FIGURE 8. Fields of the symmetric part of the linear term (left) and the quadratic term (middle), and the strange attractor (right) of the Lorenz system (7.1) for Lorenz's choice of system parameters.

for positive parameters σ , ρ and β . This system is of form (4.1) with $\mathbf{c} = \mathbf{0}$, $Q^{(1)} = 0$ and

$$L = \begin{bmatrix} -\sigma & \sigma & 0 \\ \rho & -1 & 0 \\ 0 & 0 & -\beta \end{bmatrix}, \quad Q^{(2)} = \begin{bmatrix} 0 & 0 & -\frac{1}{2} \\ 0 & 0 & 0 \\ -\frac{1}{2} & 0 & 0 \end{bmatrix}, \quad Q^{(3)} = \begin{bmatrix} 0 & \frac{1}{2} & 0 \\ \frac{1}{2} & 0 & 0 \\ 0 & 0 & 0 \end{bmatrix}. \quad (7.2)$$

In particular, the quadratic term is energy preserving. For Lorenz's choice of the parameters

$$\sigma = 10, \quad \rho = 28, \quad \beta = 8/3 \quad (7.3)$$

the solution is characterised by a strange attractor. However it is known, that the solution is long-term bounded. A trapping region of ellipsoidal form can be found via a Lyapunov function (Swinnerton-Dyer 2001).

Because there are positive and negative eigenvalues of L_S , there exist directions of positive and of negative energy growth K . However, via the quadratic term the trajectories are deflected from directions of positive energy growth to directions of negative energy growth, stabilising the resulting strange attractor (see figure 8).

The directions of energy growth and the symmetry axes of the quadratic term do not coincide. The dynamics of the system is dominated by the quadratic term in case of large deviations from the origin and far enough from fixed points of the quadratic term at the two poles and the equator. Hence, the boundedness of the system is determined by the accumulation of energy growth along the trajectories of the quadratic term crossing areas of negative and positive growth. The set of points with a vanishing quadratic term has to be investigated separately, leading to an investigation of the linear term.

In the following, long-term boundedness is shown with the criterion of theorem 1. After the translation employing $\mathbf{m} = [0, 0, \rho + \sigma]^\top$ and invoking (4.6), the symmetric part of the transformed system is equal to

$$A_S = \begin{bmatrix} -\sigma & 0 & 0 \\ 0 & -1 & 0 \\ 0 & 0 & -\beta \end{bmatrix}.$$

The negative definiteness of the matrix A_S proofs the existence of a monotonically attracting trapping region. Following theorem 1 further, one of these regions is given by the closed ball $B(\mathbf{m}, R_m)$ with $R_m = \beta(\rho + \sigma)/\sqrt{\sigma}$ in case of $\sigma > \beta > 1$. For Lorenz's choice of parameters (7.3), the trapping region is given by $B(\mathbf{m}, R_m) \approx B([0, 0, 38]^\top, 32)$. Hence, the complete strange attractor is situated inside of the ball B . It can be shown that the Lorenz system represents a prototype of the dynamics illustrated in figure 3 via further computation of the ellipsoid E using (3.12). For large times the trajectories of

the Lorenz system are pushing the boundary of the ellipsoid through and are alternately repelling from and attracting to \mathbf{m} .

8. Conclusions and future directions

We consider linear-quadratic dynamical systems and propose a criterion which is sufficient for long-term boundedness and necessary for globally stable attractor behaviour. For the first time, a straight-forward procedure (see figure 4) can discriminate between physical and unphysical behaviour for a generic class of Galerkin models with quadratic nonlinearity. The key enabler is a generalisation of Lyapunov’s direct method for identification of monotonically attracting trapping regions. These regions represent a more accessible property than the attractor property: the existence of monotonically attracting trapping regions is based solely on eigenvalue computations of linear combinations of system intrinsic matrices.

One distinct benefit is given for the model calibration and model reduction: unphysical systems can be identified a priori. One can avoid the computational burden of integration of the dynamical systems needed for a comprehensive set of system parameters and a large set of initial conditions.

Similarly, control laws which lead to unphysical nonlinear dynamical behaviour can be rejected a priori. A straight-forward control design is enabled via the design of monotonically attracting trapping regions. In the appendix section C, the respective control design is detailed for state stabilisation and for attractor control.

The criterion is applied to reduced-order models like the Galerkin models for a cylinder wake (Noack *et al.* 2003), the Lorenz system, and modifications to show long-term boundedness or indicate unboundedness (see table 1). Furthermore the capability of the criterion to reduce complexity for parameter identification is demonstrated for the Trefethen-Reddy system. Here, a Galerkin system is identified, reproducing the bootstrapping phenomenon observed in Trefethen *et al.* (1993).

The proposed methods are generalisable to Galerkin systems of larger dimensions in a straight-forward manner. Such systems may originate, for instance, from computational fluid dynamics. The numerical realisation of the criterion is only restricted by the current state of the art of the numerical linear algebra and multidimensional optimisation.

Acknowledgements

The authors acknowledge the funding and excellent working conditions of the Chaire d’Excellence ‘Closed-loop control of turbulent shear flows using reduced-order models’ (TUCOROM) of the French Angence Nationale de la Recherche (ANR) hosted by Institute PPRIME. We appreciate valuable stimulating discussions with Markus Abel, Laurent Cordier, Eurika Kaiser, Jean-Charles Laurentie, Marek Morzyński, Robert Niven, Vladimir Parezanovic, Jörn Sesterhenn, Marc Segond, and Andreas Spohn as well as the support by the Deutsche Forschungsgemeinschaft (DFG) under grants NO 258/1-1, NO 258/2-3, SCHL 586/1-1 and SCHL 586/2-1. We are grateful for outstanding computer and software support from Martin Franke and Lars Oergel.

REFERENCES

AAMO, O. M. & KRSTIĆ, M. 2002 *Flow Control by Feedback: Stabilization and Mixing*. Springer-Verlag, London.

Class 1 systems	Class 2 systems	Class 3 systems
9-mode Galerkin system (5.5) for the cylinder wake, mean-field system (5.1)	8-mode Galerkin system (5.5) for the cylinder wake	
Lorenz system (7.1)	modification (B 4) of Lorenz system for $\alpha_1 \geq 0$	modification (B 4) of Lorenz system for $\alpha_1 < 0$
'example system' (3.1)	'inversed example system' (B 1)	
modification (6.2) of the Trefethen-Reddy system for $\theta = 0, \pi/2$	modification (6.2) of the Trefethen-Reddy system for $\theta \neq 0, \pi/2$	
	Rikitake system (B 7)	
	Hamiltonian systems	

TABLE 1. Classification of the investigated dynamical systems employing the categories introduced in figure 4.

- BALAJEWICZ, M., DOWELL, E. & NOACK, B. R. 2013 Low-dimensional modelling of high-Reynolds-number shear flows incorporating constraints from the Navier-Stokes equation. *J. Fluid Mech.* **729**, 285–308.
- BOBERG, L. & BROSA, U. 1988 Onset of turbulence in a pipe. *Z. Naturforsch. A* **43**, 697–726.
- BOURGEOIS, J., NOACK, B. R. & MARTINUZZI, R. 2013 Generalised phase average with applications to sensor-based flow estimation of the wall-mounted square cylinder wake. Accepted for publication in *Journal of Fluid Mechanics*.
- CAZEMIER, W., VERSTAPPEN, R. W. C. P. & VELDMAN, A. E. P. 1998 Proper orthogonal decomposition and low-dimensional models for driven cavity flows. *Phys. Fluids* **7**, 1685–1699.
- CORDIER, L., NOACK, B. R., DAVILLER, G., LEHNASCH, G., TISSOT, G., BALAJEWICZ, M & NIVEN, R. 2013 Control-oriented model identification strategy. *Exp. Fluids* **54**, 1580.
- DEANE, A. E., KEVREKIDIS, I. G., KARNIADAKIS, G. E. & ORSZAG, S. A. 1991 Low-dimensional models for complex geometry flows: Application to grooved channels and circular cylinders. *Phys. Fluids A* **3**, 2337–2354.
- DRAZIN, P. G. & REID, H. W. 1981 *Hydrodynamic stability*. Cambridge University Press, Cambridge.
- FLETCHER, C. A. J. 1984 *Computational Galerkin Methods*. Springer, New York.
- GALDI, G. P. & PADULA, M. 1990 A new approach to the energy theory in the stability of fluid motion. *Arch. Rational Mech. Anal.* **22**, 163–184.
- GALLETI, G., BRUNEAU, C. H., ZANNETTI, L. & IOLLO, A. 2004 Low-order modelling of laminar flow regimes past a confined square cylinder. *J. Fluid Mech.* **503**, 161–170.
- GERHARD, J., PASTOOR, M., KING, R., NOACK, B. R., DILLMANN, A., MORZYŃSKI, M. & TADMOR, G. 2003 Model-based control of vortex shedding using low-dimensional Galerkin models. *AIAA-Paper* **2003-4262**.
- GERSHENFELD, N. 2006 *The Nature of Mathematical Modeling*. Cambridge University Press, Cambridge.
- GORIELY, A. & HYDE, C. 1998 Finite-time blow up in dynamical systems. *Phys. Lett. A* **250**, 311–318.
- GUCKENHEIMER, J. & HOLMES, P. 1986 *Nonlinear Oscillations, Dynamical Systems, and Bifurcations of Vector Fields*. Springer, New York.
- HOLMES, P., LUMLEY, J. L., BERKOOZ, G. & ROWLEY, C. W. 1998 *Turbulence, Coherent*

- Structures, Dynamical Systems and Symmetry*. Cambridge University Press, Cambridge, 2nd edition.
- JOSEPH, D. D. 1976 *Stability in fluid motions I, II*. Springer Tracts in Natural Philosophy **27–28**, Springer-Verlag, New York.
- KHALIL, H. K. 2002 *Nonlinear Dynamics*. Dover Publications, New York.
- KIM, J. & BEWLEY, T. 2007 A linear systems approach to flow control. *Ann. Rev. Fluid Mech.* **39**, 383–417.
- KOLDA, T. G. & BADER, B. W. 1998 Tensor decompositions and applications. *SIAM Rev.* **51**(3), 455–500.
- LADYŽHENSKAYA, O. A. 1963 *The Mathematical Theory of Viscous Incompressible Flow*. Gordon and Breach, New York.
- LYAPUNOV, A. M. 1892 *Stability of Motion*. Academic Press, London, New York.
- MCCOMB, W. D. 1991 *The Physics of Fluid Turbulence*. Clarendon Press, Oxford.
- MEISS, J. D. 2007 *Differential Dynamical Systems*. Series 'Monographs on Mathematical Modelling and Computation' **14**, Society for Industrial and Applied Mathematics, Philadelphia.
- NOACK, B. R. & FASEL, H. 1994 A global stability analysis of the steady and periodic cylinder wake. *J. Fluid Mech.* **270**, 297–330.
- NOACK, B. R., AFANASIEV, K., MORZYŃSKI, M., TADMOR, G. & THIELE, F. 2003 A hierarchy of low-dimensional models for the transient and post-transient cylinder wake. *J. Fluid Mech.* **497**, 335–363.
- NOACK, B. R., PAPAS, P. & MONKEWITZ, P. A. 2005 The need for a pressure-term representation in empirical Galerkin models of incompressible shear flows. *J. Fluid Mech.* **523**, 339–365.
- NOACK, B. R., SCHLEGEL, M., AHLBORN, B., MUTSCHKE, G., MORZYŃSKI, M., COMTE, P. & TADMOR, G. 2008 A finite-time thermodynamics of unsteady fluid flows. *J. Non-Equilib. Thermodyn.* **33** (2), 103–148.
- NOACK, B. R., SCHLEGEL, M., MORZYŃSKI, M. & TADMOR, G. 2010 System reduction strategy for Galerkin models of fluid flows. *Int. J. Numer. Meth. Fluids* **63**, 231–248.
- NOACK, B. R., MORZYŃSKI, M. & TADMOR, G. 2011 *Reduced-Order Modelling for Flow Control*. Series 'CISM International Centre for Mechanical Sciences' **528**, Springer, Wien, New York.
- REMPFER, D. & FASEL, H. F. 1994 Dynamics of three-dimensional coherent structures in a flat-plate boundary layer. *J. Fluid Mech.* **275**, 257–283.
- RUMMLER, B. & NOSKE, A. 1998 Direct Galerkin Approximation of Plane-Parallel-Couette and Channel Flows by Stokes Eigenfunctions. *Notes Numer. Fluid Mech.* **64**, 3–19.
- RUMMLER, B. 2000 Zur Lösung der instationären inkompressiblen Navier-Stokesschen Gleichungen in speziellen Gebieten (transl: On the solution of the incompressible Navier-Stokes equations in some domains). *Habilitation thesis*, Fakultät für Mathematik, Otto-von-Guericke-Universität, Magdeburg.
- SAMIMY, M., DEBIASI, M., CARABALLO, E., SERRANI, A., YUAN, X., LITTLE, J. & MYATT, J. 2010 Feedback control of subsonic cavity flows using reduced-order models. *J. Fluid Mech.* **579**, 315–346.
- SCHLEGEL, M., NOACK, B. R., COMTE, P., KOLOMENSKIY, D., SCHNEIDER, K., FARGE, M., SCOUTEN, J., LUCHTENBURG, D. M., & TADMOR, G. 2009 Reduced-order modelling of turbulent jets for noise control. In BRUN, C., JUVÉ, D., MANHART, M., MUNZ, C.-D. (editors), *Numerical Simulation of Turbulent Flows and Noise Generation*, Series 'Notes on Numerical Fluid Mechanics and Multidisciplinary Design (NNFM)' **104**, Springer-Verlag, 3–27.
- SCHLEGEL, M., NOACK, B. R., JORDAN, P., DILLMANN, A., GRÖSCHEL, E., SCHRÖDER, W., WEI, M., FREUND, J. B., LEHMANN, O. & TADMOR, G. 2012 On least-order flow representations for aerodynamics and aeroacoustics. *J. Fluid Mech.* **697**, 367–398.
- SCHLICHTING, H. 1968 *Boundary-layer theory*. McGraw-Hill, 3rd english edition.
- SCHMID, P. J. & HENNINGSON, D. S. 2001 *Stability and Transition in Shear Flows*. Applied Mathematical Sciences **142**, Springer, New York.
- SIPP, D., MARQUET, O., MELIGA, P. & BARBAGALLO, A. 2010 Dynamics and control of global instabilities in open flows: a linearized approach. *Appl. Mech. Rev.* **63**, 030801.
- SIRISUP, S. & KARNIADAKIS, G. E. 2004 A spectral viscosity method for correcting the long-term behavior of POD models. *J. Comp. Phys.* **194**, 92–116.

- STRAUGHAN, B. 2004 *The Energy Method, Stability and Nonlinear Convection*. Applied Mathematical Sciences **94**, 2nd ed., Springer-Verlag, New York.
- SWINNERTON-DYER, P. 2000 A note on Liapunov's method. *Dynam. Stabil. Syst.* **15**, 3–10.
- SWINNERTON-DYER, P. 2001 Bounds for trajectories of the Lorenz equations: an illustration of how to choose Liapunov functions. *Phys. Lett. A* **281**, 161–167.
- TREFETHEN, L. N., TREFETHEN, A. E., REDDY, S. C. & DRISCOLL, T. A. 1993 *Hydrodynamic stability without eigenvalues*. *Science* **261**, 578–584.
- TREFETHEN, L. N. & EMBREE, M. 2005 *Spectra and Pseudospectra*. Princeton University Press, New Jersey.
- WEI, M. & ROWLEY, C. W. 2009 Low-dimensional models of a temporally evolving free shear layer. *J. Fluid Mech.* **618**, 113–134.
- WILLCOX, K. & MEGRETSKI, A. 2005 Fourier Series for Accurate, Stable, Reduced-Order Models in Large-Scale Applications. *SIAM J. Sci. Comput.* **26**(3), 944–962.

Appendix A. Boundary conditions for the preservation property of the quadratic term

In this section, property (2.4) is derived for a large class of boundary conditions. The energy preservation of the quadratic term it is known for periodic boundary conditions (see, e.g. McComb 1991; Holmes *et al.* 2012) and for stationary Dirichlet conditions (Rummler 2000). Here, we extend the range of validity also for open shear flows.

We assume an incompressible flow in a stationary domain Ω with Dirichlet, periodic or uniform free-stream conditions. $\xi \in \Omega$ represents the physical location. The boundary of the domain is denoted by $\partial\Omega$.

Starting point are the quadratic Galerkin system coefficients corresponding to the convective Navier-Stokes term (see, e.g., equation (20) of the chapter ‘Galerkin method for Nonlinear Dynamics’ in Noack *et al.* 2011):

$$\tilde{q}_{ijk} := - \int_{\Omega} \mathbf{u}_i^{\top} \nabla \cdot (\mathbf{u}_j \mathbf{u}_k^{\top}) d\xi. \quad (\text{A } 1)$$

The symmetry (2.3) of the Galerkin system coefficients q_{ijk} originated from the symmetrisation

$$q_{ijk} = \frac{1}{2} (\tilde{q}_{ijk} + \tilde{q}_{ikj}). \quad (\text{A } 2)$$

It follows that equation (2.4) is equivalent to

$$\tilde{q}_{ijk} + \tilde{q}_{ikj} + \tilde{q}_{jik} + \tilde{q}_{jki} + \tilde{q}_{kij} + \tilde{q}_{kji} = 0, \quad i, j, k = 1, \dots, N. \quad (\text{A } 3)$$

Equation (A 1) is transformed by partial integration:

$$\begin{aligned}
\tilde{q}_{ijk} &= - \int_{\Omega} \mathbf{u}_i \left(\sum_{\beta=1}^3 u_j^{\beta} \frac{\partial}{\partial \xi_{\beta}} \mathbf{u}_k + \underbrace{(\nabla \cdot \mathbf{u}_j)}_{=0} \mathbf{u}_k \right) d\xi & (\text{A 4}) \\
&= - \int_{\Omega} \sum_{\alpha,\beta=1}^3 \left(u_i^{\alpha} u_j^{\beta} \frac{\partial}{\partial \xi_{\beta}} u_k^{\alpha} \right) d\xi, \\
&= - \int_{\Omega} \sum_{\alpha,\beta=1}^3 \left(\frac{\partial}{\partial \xi_{\beta}} (u_i^{\alpha} u_j^{\beta} u_k^{\alpha}) - u_k^{\alpha} \frac{\partial}{\partial \xi_{\beta}} (u_i^{\alpha} u_j^{\beta}) \right) d\xi, \\
&= - \int_{\Omega} \nabla \cdot ((\mathbf{u}_i \mathbf{u}_k) \mathbf{u}_j) d\xi + \int_{\Omega} (\mathbf{u}_i \mathbf{u}_k) \underbrace{\nabla \cdot \mathbf{u}_j}_{=0} d\xi + \int_{\Omega} \sum_{\alpha,\beta=1}^3 u_k^{\alpha} u_j^{\beta} \frac{\partial}{\partial \xi_{\beta}} u_i^{\alpha} d\xi, \\
&= - \oint_{\partial\Omega} (\mathbf{u}_i \mathbf{u}_k) \mathbf{u}_j \boldsymbol{\eta} dS - \tilde{q}_{kji}, & (\text{A 5})
\end{aligned}$$

where $\boldsymbol{\eta}$ denotes the unit outward normal at the surface $\partial\Omega$ of the considered domain Ω . Here, the incompressibility of the modes $\nabla \cdot \mathbf{u}_i = 0$, $i = 1, \dots, N$, is derived from the postulated incompressibility of the flow $\nabla \cdot \mathbf{u}$ exploiting the linearity of the Galerkin approximation (2.1) and of the divergence operator.

Let us assume vanishing surface integrals,

$$\oint_{\partial\Omega} (\mathbf{u}_i \mathbf{u}_j) \mathbf{u}_k = 0, \quad i, j, k = 1, \dots, N. \quad (\text{A 6})$$

Then, (A 5) and (A 6) imply

$$\tilde{q}_{ijk} = -\tilde{q}_{kji}, \quad i, j, k = 1, \dots, N. \quad (\text{A 7})$$

The energy preservation of the original and symmetrised quadratic terms, i.e. (2.4) and (A 3), can easily be derived from (A 7).

In the following, conditions for vanishing surface integrals (A 6) are determined. (A 6) has been shown to vanish for stationary Dirichlet conditions, implying the no-slip condition for all modes $\mathbf{u}_i \equiv \mathbf{0}$ at the boundary (see, e.g. Rummler 2000). Similarly straight-forward is the proof for periodic boundary conditions (see, e.g. McComb 1991; Holmes *et al.* 2012). Both boundary conditions may be combined, like in plane parallel Couette and Poiseuille channel flows (Rummler & Noske 1998) or in Hagen-Poiseuille flow (Boberg & Brosa 1988).

The proof for free-stream conditions at infinity is more challenging, as it requires certain far-wake properties of the flow. We consider flows in infinite domains around obstacles of finite extend. The integrals (A 6) vanish if the velocity rapidly decreases for large distances from the origin. As examples of free turbulent shear flows, nominally two-dimensional cylinder wakes, two-dimensional jets and three-dimensional circular jets are considered. Here, it is easily shown that a sequence of integrals (A 6) over surfaces of concentric balls Ω_R converge to zero, if their radii R converge to infinity. As centre of the balls Ω_R , the centre of the cylinder or the centre of the nozzle exit might be employed. An upper bound of the absolute values of the integrals is estimated via the radius, the dimension $D = 2, 3$ of the flow configuration and the centre line (fluctuation) velocity u_c in streamwise direction.

The surface integral over the sphere Ω_R reads

$$\begin{aligned} \left| \oint_{\partial\Omega_R} (\mathbf{u}_i \mathbf{u}_j) \mathbf{u}_k \boldsymbol{\eta} dS \right| &\leq \oint_{\partial\Omega_k} |\mathbf{u}_i| |\mathbf{u}_j| |\mathbf{u}_k| |\boldsymbol{\eta}| dS, \\ &\leq \sup |\mathbf{u}_i| \sup |\mathbf{u}_j| \sup |\mathbf{u}_k| |\Omega_R|, \\ &\propto u_c(R)^3 R^{D-1}. \end{aligned} \quad (\text{A } 8)$$

Following Schlichting (1968), the centre line velocity is decreasing with radius R via

$$u_c(R) \propto R^\kappa \quad (\text{A } 9)$$

where the decay rate κ is equal to $-1/2$ for two-dimensional wakes and jets, and $\kappa = -1$ for the circular jet. Employing the estimate (A 8), in summary, there is a decrease of the absolute value of the integrals (A 6) with $R^{-1/2}$ for two-dimensional wakes and jets and with R^{-1} for the three-dimensional circular jet. Hence, the integrals converge to zero for $R \rightarrow \infty$ leading to vanishing integrals over the infinite domain.

In conclusion, an intrinsic preservation property (2.4) exists for Galerkin systems of configurations with corresponding boundary conditions, e.g. flows around obstacles like spheres, cylinders and airfoils, in uniform stream as well as many internal flows.

Appendix B. Examples of unboundedness, vanishing nonlinearity and semidefiniteness

In this section, dynamical systems (2.2) are discussed which do not obey the criterion for boundedness of theorem 1. The examples include a modification of the two-dimensional system (3.1) (subsection B.1), modified Lorenz equations (subsection B.2), and the Rikitake system (subsection B.3).

B.1. Two-dimensional system of ordinary differential equations

A first example for divergent dynamical behaviour is given from the time inversion $t \mapsto -t$ of (3.1). The resulting system has propagators of opposite sign and reads

$$\frac{dx_1}{dt} = x_1 - x_2^2, \quad (\text{B } 1a)$$

$$\frac{dx_2}{dt} = -x_2 + x_1 x_2, \quad (\text{B } 1b)$$

where

$$\mathbf{c} = \begin{bmatrix} 0 \\ 0 \end{bmatrix}, L = \begin{bmatrix} 1 & 0 \\ 0 & -1 \end{bmatrix}, \mathbf{Q}^{(1)} = \begin{bmatrix} 0 & 0 \\ 0 & -1 \end{bmatrix}, \mathbf{Q}^{(2)} = \begin{bmatrix} 0 & \frac{1}{2} \\ \frac{1}{2} & 0 \end{bmatrix}. \quad (\text{B } 2)$$

The long-term behaviour of system (B 1) is investigated employing the criterion of theorem 1. Invoking (4.6) and employing the matrices (B 2), the symmetric part of the shift transformed system is determined to be

$$A_S = \begin{bmatrix} 1 & -m_2/2 \\ -m_2/2 & m_1 - 1 \end{bmatrix}.$$

The larger eigenvalue of A_S

$$\lambda_1 = \frac{1}{2} \left(m_1 + \sqrt{(2 - m_1)^2 + m_2^2} \right)$$

is positive: $\lambda_1 \geq 1$ is concluded from $|2 - m_1| \geq 2 - m_1$ because

$$m_1 + \sqrt{(2 - m_1)^2 + m_2^2} \geq m_1 + |2 - m_1| \geq 2. \quad (\text{B } 3)$$

Hence, a monotonically attracting trapping region and a globally stable attractor do not exist. By numerical system integration, a divergent behaviour to infinity is observed for large times.

B.2. Modified Lorenz system

Similarly, the following modification of the Lorenz system

$$\frac{dx_1}{dt} = \alpha_1 x_1, \quad (\text{B } 4a)$$

$$\frac{dx_2}{dt} = \alpha_2 x_2 - x_1 x_3, \quad (\text{B } 4b)$$

$$\frac{dx_3}{dt} = \alpha_3 x_3 + x_1 x_2, \quad (\text{B } 4c)$$

with $-\infty < \alpha_1, \alpha_2, \alpha_3 < \infty$ is considered for investigation of existence of monotonically attracting trapping regions and of globally stable attractors. From equation (4.6) we get

$$A_S = \begin{bmatrix} \alpha_1 & -m_3/2 & m_2/2 \\ -m_3/2 & \alpha_2 & 0 \\ m_2/2 & 0 & \alpha_3 \end{bmatrix}.$$

Independently of the choice of \mathbf{m} , the sum of the three eigenvalues of A_S is equal to the constant trace of A_S , i.e. the mean value $\gamma = (\lambda_1 + \lambda_2 + \lambda_3)/3$ is constant. The eigenvalues are increasingly separated with growing $|m_2|$, $|m_3|$ which can be seen from the dispersion of the eigenvalues

$$\frac{1}{3} \sum_{i=1}^3 (\lambda_i - \gamma)^2 = \frac{1}{3} \left(\sum_{i=1}^3 \lambda_i^2 \right) - \gamma^2 = f(\alpha_1, \alpha_2, \alpha_3) + \frac{m_2^2 + m_3^2}{6}. \quad (\text{B } 5)$$

For derivation of (B 5), Vieta's formula for the characteristic polynomial of A_S

$$(\lambda - \alpha_1)(\lambda - \alpha_2)(\lambda - \alpha_3) - \frac{m_2^2}{4}(\lambda - \alpha_2) - \frac{m_3^2}{4}(\lambda - \alpha_3)$$

is employed, which yields

$$\frac{3}{2}\gamma^2 - \frac{1}{2}(\lambda_1^2 + \lambda_2^2 + \lambda_3^2) = \lambda_1\lambda_2 + \lambda_2\lambda_3 + \lambda_1\lambda_3 = \alpha_1\alpha_2 + \alpha_2\alpha_3 + \alpha_1\alpha_3 - \frac{m_2^2 + m_3^2}{4}.$$

From the increased dispersion of the eigenvalues and the preservation of the mean value, the following can be concluded: If one of the three growth rates α_i is positive, then for each \mathbf{m} there is always at least one λ_i positive as well. Following theorem 1, a monotonically attracting trapping region does not exist in that case. This result is easily validated considering the dynamics in case that one eigenvalue is positive. For $\alpha_1 > 0$, the variable x_1 is diverging to infinity for large times. For $\alpha_1 < 0$ and large times the quadratic term is small compared to the linear term and the variable x_i with positive α_i is diverging to infinity. If $\alpha_1 = 0$, x_1 is constant in time for each initial value, i.e. a monotonically trapping region does not exist either.

In the case $\alpha_1 < 0$, the nonlinear term of the system (B 4) is vanishing for large times. Invoking theorem 2, under action of an additional antisymmetric part, there might exist globally attracting trapping regions or fixed points which are not monotonically

attracting. One example with an additional antisymmetric linear term is

$$\frac{dx_1}{dt} = \alpha_1 x_1, \quad (\text{B } 6a)$$

$$\frac{dx_2}{dt} = \alpha_2 x_2 - x_3 - x_1 x_3, \quad (\text{B } 6b)$$

$$\frac{dx_3}{dt} = \alpha_3 x_3 + x_2 + x_1 x_2. \quad (\text{B } 6c)$$

The analysis for a monotonically attracting region is de facto the same like in system (B 4). However, if $\alpha_1 < 0$, the application of linear theory is enabled by the vanishing of the nonlinear term for large times. Only the evolution equations for x_2 and x_3 are considered while the nonlinear term is neglected. Here, $[x_2, x_3]^\top = [0, 0]^\top$ is a globally stable fixed point, if and only if the real parts of the eigenvalues of $\begin{bmatrix} \alpha_2 & -1 \\ 1 & \alpha_3 \end{bmatrix}$ are negative-valued. In conclusion, in case of a vanishing nonlinearity, linear analyses are needed in addition for a complete analysis of the long-term boundedness of the system.

B.3. The Rikitake system

The criterion of theorem 1 cannot be generalised from negative definite matrices A_S to negative semidefinite matrices A_S in a straight-forward manner. As a corresponding example, a modified Rikitake system

$$\frac{dx_1}{dt} = -\nu x_1 + x_2 x_3, \quad (\text{B } 7a)$$

$$\frac{dx_2}{dt} = -\alpha x_1 - \nu x_2 + x_1 x_3, \quad (\text{B } 7b)$$

$$\frac{dx_3}{dt} = \theta - \omega x_1 x_2, \quad (\text{B } 7c)$$

is utilised with the positive parameters ν and α (Goriely & Hyde 1998). In the traditional Rikitake system, $\theta = 1$ and $\omega = 1$ are chosen. Here ω is set to $\omega = 2$ to fulfil the postulation (2.3). From similar analyses like above, the positive semidefiniteness of the largest eigenvalue, i.e. $\lambda_1 \geq 0$, of A_S can be shown. In the following, $\mathbf{m} = [0, 0, \alpha/2]^\top$ is considered, where $\lambda_1 = 0$ and $\lambda_2 = \lambda_3 = -\nu$ because

$$A_S = \begin{bmatrix} -\nu & 0 & 0 \\ 0 & -\nu & 0 \\ 0 & 0 & 0 \end{bmatrix}.$$

We leave $\theta = 1$ at first. Here, it is known that there is a simple solution $\mathbf{x} = [0, 0, t]^\top$ which is diverging to infinity for large times. However for $\theta = 0$, long-term boundedness is immediately ensured invoking the evolution equation (3.4) for the chosen A_S and $\mathbf{d} = \mathbf{0}$: the energy $K_{\mathbf{m}}$ cannot grow in any direction. This means that for negative semidefinite A_S additional information, e.g. of the constant term might be crucial for long-term boundedness analyses.

Appendix C. Large-deviation and attractor control

C.1. General considerations

In this section, applications of the criterion of section 4 for control design are sketched.

For control, the term $B\mathbf{b}(t)$ is added to the right side of the Galerkin system (4.1)

leading to

$$\frac{d\mathbf{x}}{dt} = \mathbf{c} + L\mathbf{x} + B\mathbf{x} + \left[\mathbf{x}^\top Q^{(1)}\mathbf{x}, \dots, \mathbf{x}^\top Q^{(N)}\mathbf{x} \right]^\top + B\mathbf{b} \quad (\text{C1})$$

with the input matrix B and the input vector $\mathbf{b} = \mathbf{b}(t)$. Let us assume full-state feedback with constant, linear and quadratic terms

$$\mathbf{b} = \mathbf{c}^b + L^b\mathbf{x} + \left[\mathbf{x}^\top Q^{b(1)}\mathbf{x}, \dots, \mathbf{x}^\top Q^{b(N)}\mathbf{x} \right]^\top \quad (\text{C2})$$

with the free coefficients in \mathbf{c}^b , L^b and $Q^{b(i)}$. The actuation term reads

$$B\mathbf{b}(t) = \mathbf{c}^g + B^g\mathbf{x} + \left[\mathbf{x}^\top Q^{g(1)}\mathbf{x}, \dots, \mathbf{x}^\top Q^{g(N)}\mathbf{x} \right]^\top, \quad (\text{C3})$$

introducing the feedback vector \mathbf{c}^g , the feedback matrix L^g , and the symmetric matrices $Q^{g(i)}$ for the quadratic term of feedback. We request that the control law (C2) is chosen to respect the energy preservation property

$$q_{jk}^{g(i)} + q_{ik}^{g(j)} + q_{ij}^{g(k)} = 0, \quad i, j, k = 1, \dots, N. \quad (\text{C4})$$

In summary, the actuated system reads

$$\frac{d\mathbf{x}}{dt} = \mathbf{c}^a + L^a\mathbf{x} + \left[\mathbf{x}^\top Q^{a(1)}\mathbf{x} + \mathbf{x}^\top Q^{a(N)}\mathbf{x} \right]^\top, \quad (\text{C5})$$

where $\mathbf{c}^a = \mathbf{c} + \mathbf{c}^g$, $L^a = L + L^g$, and $Q^{a(i)} = Q^{(i)} + Q^{g(i)}$, $i = 1, \dots, N$. The controlled system is of form (4.1) and thus contained in the class of dynamical systems considered in this paper. That's why the long-term behaviour of the corresponding dynamics can be investigated by the criterion of theorem 1. In control design, the choice of the parameters \mathbf{c}^b , L^b and $Q^{b(i)}$, $i = 1, \dots, N$, is restricted by constraints implied by the input matrix L^g .

Two tasks are pursued here

(a) Large-deviation control: The purpose of this part is twofold. One goal is the modification of the parameters of system (4.1) such that the existence of a monotonically attracting trapping region is ensured. On the other hand, artefacts like blow-ups in model-based control design are precluded a priori.

(b) Attractor control: Target is the manipulation of statistical attractor moments. Thereto, in this paper, tools are provided to design the volume and the location of monotonically attracting trapping regions. In one extreme case, on which is focused here, a globally attracting fixed point is designed, i.e. the attractor mean is equal to a fixed point and the higher central moments are zero. Focus of large deviation control is the identification or creation of monotonically attracting trapping regions. This can be achieved as described in section 4.

As one extreme case of attractor control, we assume a constant actuation, i.e. vanishing L^b and $Q^{b(i)}$. The feedback vector \mathbf{c}^g may be chosen such that each state $\mathbf{m} \in \mathcal{S}$ is a globally attracting fixed point of the feedback system. This implies

$$0 = \mathbf{c}_i^a + \sum_{j=1}^N l_{ij} m_j - \sum_{j,k=1}^N q_{jk}^{(i)} m_j m_k, \quad i = 1, \dots, N. \quad (\text{C6})$$

Then, the energy $K_{\mathbf{m}}$ represents a Lyapunov function, because the linear symmetric part A_S is negative definite. The choice of the feedback vector \mathbf{c}^g might be restricted such that a globally stable fixed point is not attainable due to the constraints implied by the input matrix L^g of the flow control configuration. However even in this case, the first and second

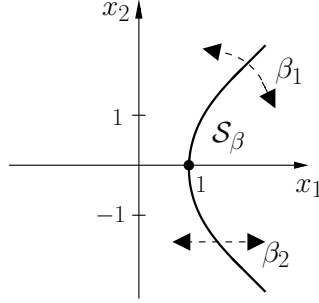


FIGURE 9. Design of the open set \mathcal{S}_β of stabilisable states at the left side of the curve. By variation of the parameters $\beta = [\beta_1, \beta_2]^\top$ of the feedback matrix L_β^g , the set \mathcal{S}_β is modified via a widening/narrowing (varying β_1) of the right opening angle of the set or a spatial shift in x_1 -direction (via varying β_2).

attractor moments can be estimated from the location and the volume of the trapping region. Thus, the moments can be manipulated by the design of the ellipsoid of energy growth given by equation (3.12). The effort of a corresponding volume force actuation for this attractor control might be large. A trade-off between the attractor scaling via choice of \mathbf{c}^g and the above discussed design of \mathcal{S} might be necessary for model-based flow control applications.

Examples for the application of large deviation and attractor control are discussed in the following.

C.2. Example for large deviation control

For large deviation control, the set \mathcal{S} of stabilisable states is analytically or numerically created and designed for the example of system (3.1) endowed with a linear feedback matrix of the family of linear symmetric matrices

$$L_\beta^g := \begin{bmatrix} \beta_1 & 0 \\ 0 & \beta_2 \end{bmatrix}. \quad (\text{C7})$$

The corresponding sets \mathcal{S}_β of stabilisable states \mathbf{m} are identified via auxiliary calculations to be

$$\mathcal{S}_\beta = \begin{cases} \{\mathbf{x} = [x_1, x_2]^\top : x_1 > 1 + \beta_2, |x_2| < 2\sqrt{1 - \beta_1}\sqrt{x_1 - 1 - \beta_2}\} & \text{for } \beta_1 < 1, \\ \emptyset & \text{for } \beta_1 \geq 1. \end{cases} \quad (\text{C8})$$

In particular, $\mathcal{S}_0 := \{\mathbf{x} = [x_1, x_2]^\top : x_1 > 1, |x_2| < 2\sqrt{x_1 - 1}\}$. Starting from \mathcal{S}_0 , the set \mathcal{S}_β is designed via variation of β as demonstrated in figure 9. If the set $\mathcal{S} = \mathcal{S}_\beta$ is not empty, the long-term dynamics of the resulting system is bounded invoking theorem 1.

In the case $\beta_1 \geq 1$, the set of stabilisable states is empty and a monotonically attracting trapping region does not exist, which is obvious considering the resulting system

$$\frac{dx_1}{dt} = (\beta_1 - 1)x_1 + x_2^2, \quad (\text{C9})$$

$$\frac{dx_2}{dt} = (1 + \beta_2)x_2 - x_1 x_2, \quad (\text{C10})$$

in the subspace of the x_1 -axis, i.e. $x_2 = 0$. It means, that the L_β^g with $\beta_1 \geq 1$ cannot be chosen to form a control with bounded system behaviour.

C.3. Example for attractor control

As attractor control example, we control the size of the monotonically attracting trapping region. The Lorenz system (7.1) is extended by a control vector $\mathbf{c}^g = \gamma [0, 0, \beta(\rho + \sigma)]^\top$ with $\gamma \in [0, 1]$ such that

$$\frac{d\mathbf{x}}{dt} = \gamma \begin{bmatrix} 0 \\ 0 \\ \beta(\rho + \sigma) \end{bmatrix} + \begin{bmatrix} -\sigma & \sigma & 0 \\ -\rho & -1 & 0 \\ 0 & 0 & -\beta \end{bmatrix} \mathbf{x} + \begin{bmatrix} 0 \\ -x_1 x_3 \\ x_1 x_2 \end{bmatrix}. \quad (\text{C } 11)$$

For $\gamma = 0$, this system is identical to the Lorenz equations (7.1). From the transformation shift of $\mathbf{m} = [0, 0, \rho + \sigma]^\top$ to the origin, the system for $\mathbf{y} = \mathbf{x} - \mathbf{m}$ is obtained:

$$\frac{d\mathbf{y}}{dt} = (\gamma - 1) \begin{bmatrix} 0 \\ 0 \\ \beta(\rho + \sigma) \end{bmatrix} + \begin{bmatrix} -\sigma & \sigma & 0 \\ -\sigma & -1 & 0 \\ 0 & 0 & -\beta \end{bmatrix} \mathbf{y} + \begin{bmatrix} 0 \\ -y_1 y_3 \\ y_1 y_2 \end{bmatrix} \quad (\text{C } 12)$$

For $\gamma = 1$ the constant part of the right side is equal to zero. Thus, the energy is a Lyapunov function and \mathbf{m} is a globally stable fixed point in this case. Generally, the equation (3.12) for the ellipsoid of positive energy growth is given in original coordinates by

$$\frac{x_1^2}{\alpha_1^2} + \frac{x_2^2}{\alpha_2^2} + \frac{(x_3 - (\rho + \sigma) + (\gamma - 1)(\rho + \sigma)/2)^2}{\alpha_3^2} = 1 \quad (\text{C } 13)$$

with the half-axes

$$\alpha_1 = (1 - \gamma) \frac{\rho + \sigma}{2\sqrt{\sigma}}, \quad \alpha_2 = (1 - \gamma) \frac{\rho + \sigma}{2}, \quad \alpha_3 = (1 - \gamma) \frac{\rho + \sigma}{2\sqrt{\beta}}. \quad (\text{C } 14)$$

Hence, the half-axes are shrinking linearly with the growth of γ . This is true as well as for the radius of the monotonically attracting trapping region given by the smallest ball with \mathbf{m} at the centre which contains the ellipsoid.

In conclusion, the attractor contained in this trapping region is shrinking, and degenerates to a fixed point for $\gamma = 1$. The first statistical moment situated in the ball is converging to \mathbf{m} for $\gamma \rightarrow 1$, the standard deviation bounded by the ball radius is converging to zero. For $\gamma \approx 0.288$ there is a transition from the strange attractor to three fixed points which converge for $\gamma \rightarrow 1$ to the monotonically stable fixed point \mathbf{m} at $\gamma = 1$. Thus, the control parameter γ defines a transition scenario between stationary and chaotic dynamical behaviour!